

Turbulence Upset and Other Studies on Jet Transports

JEROME G. THEISEN* AND JOHN HAAS†

Lockheed-Georgia Research Laboratory, Marietta, Ga.

An analytical computer simulation including coupling of control surface motions with dynamic stability modes and complete-airplane aeroelastic response in atmospheric turbulence is presented. Comparisons with the flight records recovered from a wrecked jet transport demonstrate the ability to simulate characteristics of catastrophic upsets of commercial transports in severe turbulence. Further application predicts an unusual buffet phenomenon. A digital computer automatically mechanizes an analog computer for the complete simulation. Nonlinear aerodynamics allows wing and stabilizer stall; time-dependent coefficients in the equations of motion allow variations in control deflections and gains, forward speed, and lift due to indicial delay. Compressibility effects indicate that the over-all Prandtl-Glauert correction applied to the incompressible gust-loads formula leads to conservative values of the load factor when compared to those based on the exact theory. Shock-induced stall buffet is not present in all upsets as are the gust-induced oscillations and subsequent intractability. Some basic stability parameters are shown to be inadequate at high subsonic speeds. New results characterize a gust-load factor which improves this method of accounting for unsteadiness and compressibility. Revised design criteria, including coupling with control systems and pilot response characteristics, as well as a statistical re-evaluation of gust-load data, are possible future needs.

Nomenclature

a	= normal-force-curve slope
b	= wing mean semichord
C	= aerodynamic coefficient matrix like M_4 , M_5
F	= column matrix for control motions
g	= acceleration due to gravity
K	= normalizing factor for buffet spectra; also, time constant for indicial lift-growth functions
K_g	= gust-load alleviation factor
$K_{g^{spec}}$	= $0.88 \mu \beta (5.3 + \mu \beta)$
K_G	= K_g / β
M	= Mach number
M_1, M_2, M_3	= generalized coefficient matrices of mass, damping, and stiffness, including both aerodynamic and structural terms
M_4, M_5	= aerodynamic coefficient matrices associated with circulation lag which accounts for the gradual formation of lifting pressure
M_w	= wing mass
n	= normal load factor
p	= Laplace-transformed independent variable
q, \dot{q}, \ddot{q}	= generalized coordinates, their rates and accelerations for all of the rigid and flexible modes of interest
s	= dimensionless time = $Vt/2b$
S	= wing area; also used for s in Fig. 8
t	= time
T	= aircraft transfer function
$u(s)$	= Heaviside step function
U	= derived gust velocity
V	= aircraft forward speed
w_g	= gust velocity
W	= aircraft weight
α, α_{FRL}	= angle of attack

β	= $(1 - M^2)^{1/2}$
ϵ	= induced angle of attack of the tail
μ	= mass parameter = $(W/S)/\rho b a g$
ξ	= wing vertical displacement-coordinate
ρ, ρ_0	= air density; sea-level air density
ϕ	= modified Wagner function
Φ_i, Φ_r	= input and response buffet spectra
ψ	= modified Küssner function

Introduction

IN recent years the problem of operating transport aircraft under a wide variety of rough-air conditions has received a great deal of publicity as the result of a series of dramatic flight incidents involving both military and commercial passenger jetliners. For example, in February 1963, a jetliner climbing out of a thunderstorm area near Miami crashed, killing all aboard. The pilot had reported severe turbulence. Several other incidents occurred in 1963 in which control of jetliners was temporarily lost, resulting in an extreme loss of altitude in two cases (37,000 to 12,000 ft and 19,000 to 6,000 ft) and inverted flight in a third case. In February 1964, another jetliner, climbing at 15,000 ft, suddenly plunged into Lake Pontchartrain. In all of these incidents, atmospheric turbulence was either suspected or known to be a contributing factor.

Concerned with the lack of knowledge about the conditions under which a jet transport can be "upset" (thrown out of control) while penetrating turbulence, the Lockheed-Georgia Research Laboratory sponsored an engineering project to develop and demonstrate a simulation program for studying the turbulence-penetration characteristics of swept-wing jet transports. The program includes all those features commonly known to have bearing on the penetration problem, including: dynamic aeroelastic effects on the predominantly rigid-body dynamic stability and control problem; nonlinear, time-dependent aerodynamics to account for large angle-of-attack effects into the low-speed stall regime and also shock-induced stall buffet; Mach number effects on the aerodynamics to account for compressibility at high subsonic speeds; control systems and pilot-response features to simulate maneuvering flight; both lateral and longitudinal dynamics for studying generally asymmetric flight conditions;

Presented as Paper 66-1002 at the AIAA Third Annual Meeting, Boston, Mass., November 29–December 2, 1966; submitted February 2, 1967; revision received April 19, 1968. The authors appreciate the cooperation of the Lockheed-Georgia Company's engineering staff, including G. F. Hart and T. D. R. Neil, who performed the computer programming for the effects of compressibility on gust loads and C. V. Williams, who performed the original analysis of pitchup due to shock-induced separation which occurs in high-altitude, high-speed upsets.

* Staff Scientist. Member AIAA.

† Scientist Associate. Associate Member AIAA.

and input capacity for simulating at will either random or discrete atmospheric gust conditions. Variations in weight distribution and center-of-gravity location are based on a mission analysis performed externally to the program. In simulating specific airplane configurations, use is made of prototype- or model-test data from similar jet transports to determine aerodynamic or structural dynamic coefficients when more representative values are not available. Final coefficient values are adjusted to stay within allowable combinations of load, Mach number, etc., by iteratively comparing the simulation responses with available flight records.

Purpose

The purpose of this paper is to outline the main features of the simulation program and to present results from it and from corroborative investigations. The variety of analyses includes compressibility effects on unsteady aerodynamic loads, the buffeting of flexible aircraft structures, and the simulation of jet-transport upset in turbulence. With such aeromechanical detail, a more realistic over-all dynamic simulation is possible than is usually made with multidegree-of-freedom, moving-base simulators. The number of such simulators exhibiting realism in the opinion of pilots¹ is very small, and available test time is limited and expensive. The results from the present program are intended to demonstrate the simulation of difficult problems such as upset by adhering to the rules for pilot action derived from independent human-factors studies, including those from flight tests and the 1- or 2-degree-of-freedom piloted simulators reported by the Federal Aviation Agency (FAA), NASA,¹ and the airlines.² The results should also show how the simulated buffet response compares with the flight records. Finally, a new analysis is intended to show whether or not the effect of compressibility was properly accounted for in the transient-gust part of the simulation, and also to investigate the validity and accuracy of applying the over-all Prandtl-Glauert correction to the incompressible gust-load formula.

Simulation

The aim of the program is to admit the simultaneous occurrence of all phenomena associated with a pilot-controlled penetration of severe turbulence. This means that short-period responses associated with dynamic aeroelastic response may be essential to understanding the long-period responses directly associated with an upset. For example, a pilot might suffer considerable disorientation due to the flexible dynamic response (short period). Therefore, it would be essential to an upset problem to know the level of cockpit vibration in order to interpret pilot response, even though the pilot-response range may directly affect only the longer-period rigid modes of the airplane.

The program simulates the problem of piloted maneuvering flight through an arbitrary spatial gust field at speeds ranging over most of the subsonic regime. Important features are the effects associated with compressibility, wing sweep, pilot response, the control system, positive and negative low- and high-speed stall, the gust field, and the dynamic stability and aeroelastic response characteristics of the airframe. Simultaneously occurring dynamic responses can be studied to reach a better understanding of the diverse interactions among the pilot and the various structural, aerodynamic, and control systems of an airplane which penetrates severe turbulence. Mild dynamic loading effects, such as those in various buffeting phenomena, and control system designs to alleviate gust loads can also be studied. This capability is based on the method of analysis shown in Fig. 1. Most of the basic airplane data are processed on a digital computer to produce the coefficients required for the coupled systems analysis.³ This latter analysis simulates the flight either on the digital computer or on an operational analog

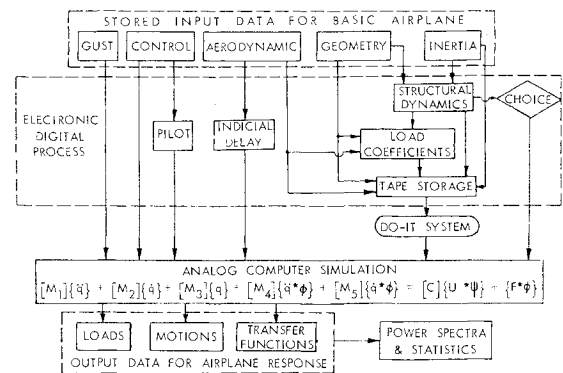


Fig. 1 Simulation program.

computer which is set up automatically from input tapes containing the coefficient data from the digital computer. A brief description of the physical considerations and analytical representations of the simulation program is in the following sections.

Structural Dynamics

Both rigid and flexible, symmetric and antisymmetric structural motions are of interest. For rigid motion such as maneuvering flight, the mass and moments of inertia are computed, allowing for all 6 degrees of freedom. For flexible motions, small amplitudes of motion are considered to occur relative to the rigid body. The usual elastic, small-amplitude vibration analysis is solved, and the structure is represented dynamically in its normal modes. All major components are idealized to an elastic-axis representation with provisions for varying sweep and dihedral. Rigid chord sections are used for the lifting surfaces. For the wing, fore and aft bending flexibility is included. An elastic beam representing the fuselage is upswept at the tail and extended along the elastic axis of the vertical stabilizer. Wing and horizontal stabilizer elastic axes sweep away from the fuselage-vertical stabilizer axis, and all engine and external-store pylons are similarly represented by elastic axes joined to the wing's elastic axis and supporting rigid distributed-mass loads. The complete-airplane normal modes are obtained from component modes by Lagrangian multiplier coupling through Lagrange's equations of motion. Control surfaces are considered only as rigid appendages affecting the inertial properties of the parent surfaces.

Aerodynamics

Compressible subsonic aerodynamics based on both steady and unsteady flow effects are used to allow for the simultaneous occurrence of both large and small disturbances. High aspect ratios are implied by the use of strip theory.

Small disturbances: In mild buffet, delay in lift-growth and compressibility effects are accounted for by using modified forms of the Wagner and Küssner functions. A single reference chord is used to express the distance traveled by all the aerodynamic strips.

Large disturbances: For strong-gust encounters, high-g maneuvers, stall buffet, and shock stall, aerodynamic coefficients such as the section lift coefficient are represented as nonlinear functions of the angle of attack α . Since α is time-dependent, the aerodynamics is thus characterized as being time-dependent and nonlinear. The angle of attack is variable from negative through positive stall; hysteresis effects as in stall buffet may be included.

Gust: Gust profiles such as turbulence are represented in the analog simulation as spatial vector fields of arbitrary amplitude variation and orientation. The digital simulation allows only the purely symmetric or purely antisymmetric transverse gust.

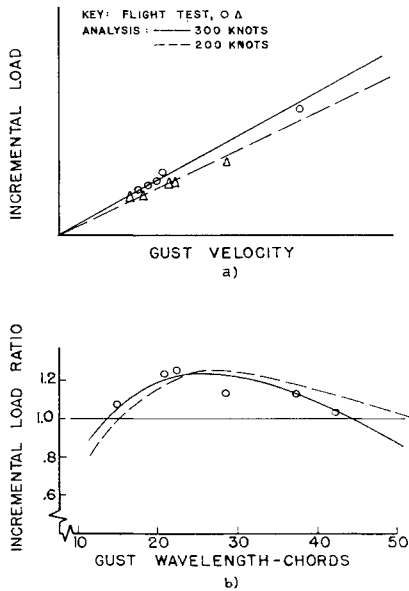


Fig. 2 Comparison with flight test.

Wing and pylon: The use of experimental values for the lift and moment coefficients in strip theory or, by the method of Ref. 4, accounts for finite span, taper, and sweep. The gradual penetration of the gust further accounts for the effect of sweep, as well as the effect of tail length. Pylons are treated as lifting surfaces. The use of empirical data accounts for interference effects.

Tail: Tail surfaces are treated as single strips. The effects of downwash and sidewash are obtained through simple approximate relationships such as the familiar formula, $\alpha_{tail} = (1 - de/d\alpha)\alpha_{wing}$. Again, interference effects are accounted for empirically.

Fuselage: The rigid-body lift and moment of the fuselage are important and therefore included.

Control surfaces: Control-surface forces are computed as incremental changes in strip angle of attack. Thus, an elevator deflection changes the effective angle of attack of the horizontal stabilizer. Such characteristics are generally nonlinear and time-dependent.

Pilot and Control System

The pilot and control system can be represented by generally nonlinear functions of the other system variables, as would occur with an autopilot or with a pilot in response to instrument readout, cockpit accelerations, or horizon changes. Or, control motions can be specified functions of time. Thrust can be included for studying this means for controlling upset and recovery. The alleviation of gust loads by means of adaptive automatic feedback control is a possible study.

Equations of Motion

The equations of motion have the form: $M_3\ddot{q} + M_2\dot{q} + M_3q + M_4(\dot{q}*\phi) + M_5(\dot{q}*\psi) = C(w\dot{q}*\psi) + (F*\phi)$, where the star implies the convolution integral. The coefficient matrices can depend on the generalized coordinates and their derivatives, making the equations highly nonlinear. Solutions are achieved by taking small increments in time and using constant coefficients which are assigned values corresponding to a linear-segment approximation to the actual time functions.

Comparison with Flight Test

Excellent agreement in the comparison of analysis and flight test is shown in Fig. 2. Incremental wing-root bending

moments vs gust velocity are plotted in Fig. 2a for two flight speeds, 240 and 300 knots. The smallness of the scatter is remarkable, since the analytical results are based on a 1-cos gust, whereas flight tests generally correspond to arbitrary gusts. Although the test data are selected for gusts most resembling a 1-cos shape, even these were very erratic.

Figure 2b shows incremental wing-root bending moments normalized by their values for the rigid airplane and plotted as a function of the gust wavelength. In spite of the difficulty in identifying gust wavelengths from the test data, the agreement is good.

Turbulence Upset

Prior to several incidents, pilots reported only moderate turbulence, which suggests that gust-induced angle of attack must be interacting with other aerodynamic or control factors to cause the final upset. Some of these factors are: 1) shock-induced boundary-layer separation, a likely cause of the violent pitching observed in the flight records because of the associated shift in the center of pressure; 2) the narrow margins between the low- and high-speed buffet boundaries at the high altitudes where several of the upsets occurred; and 3) disorientation of the pilot by turbulence, such that the pilot is unable to maintain flight within the buffet margins.

Preliminary Studies

Consider the flight record of a high-altitude, high-speed upset. The instantaneous normal-load factor is given by the record as a continuous trace with time. For a given speed, altitude, and weight, the load factor at which low- or high-speed buffet occurs is known from the buffet boundaries for a given airplane (e.g., Fig. 3). Comparison of these two load factors shows approximately the periods during which the airplane has penetrated the stall-buffet region.

Now consider an actual incident, upset A (Fig. 4). (C_L and n are equivalent for estimating stall, since $C_L = 2nW/S\rho V^2$.) The deepest stall occurs at approximately 3 min, 28 sec with load factors of more than 2 g's. The aircraft dips repeatedly in and out of the high-speed stall region (hatching in figure) at half-minute intervals. Initially diverging oscillations indicate control difficulties; however, for 1.5 min just prior to upset, the Mach number drops, allowing partial recovery and thereby reducing the stall penetrations. To reduce the positive stall buffeting, the pilot evidently pitches the airplane nose-downward, as indicated

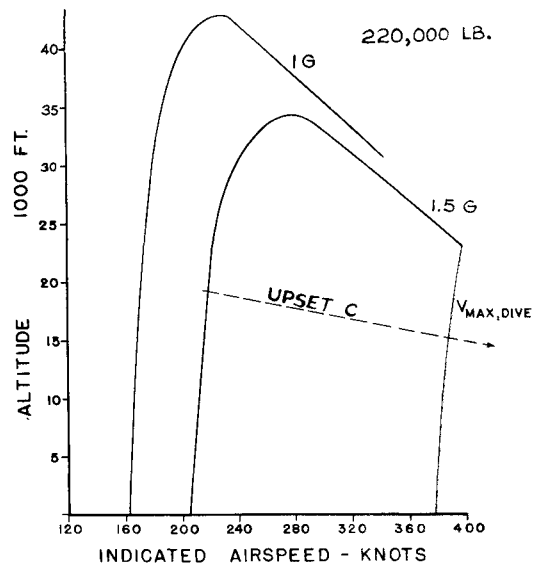
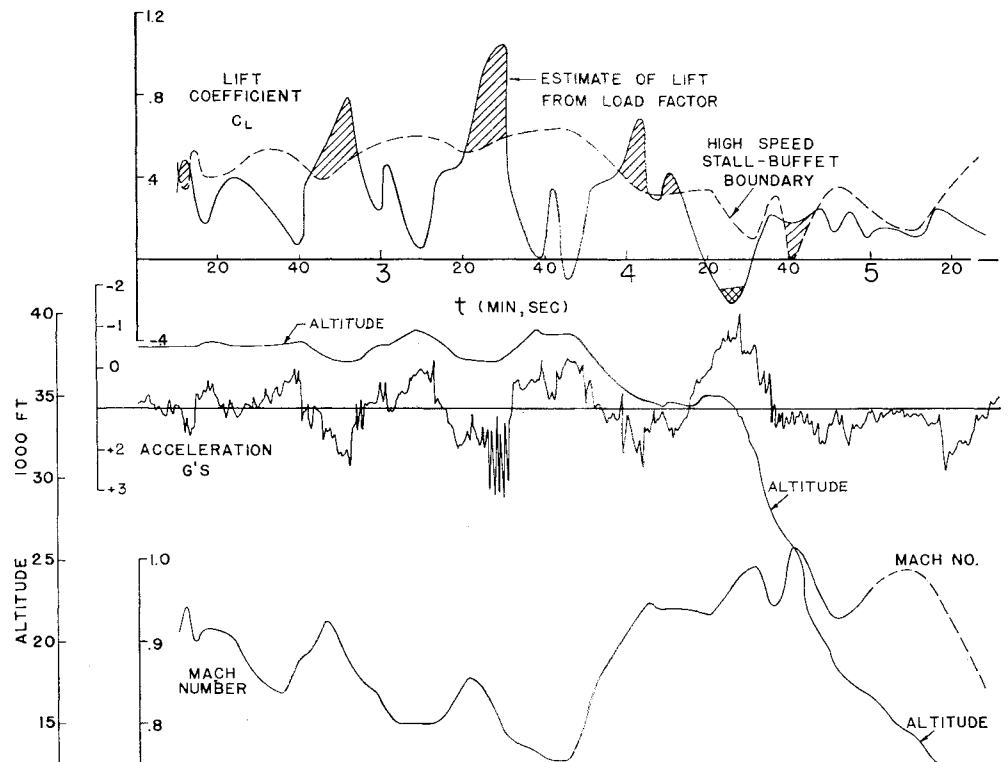


Fig. 3 Buffet boundary.

Fig. 4 Flight record of upset A.



by the subsequent loss of altitude. There follows a sharp increase in Mach number and a negative stall (cross-hatching) at 4 min, 25 sec. A further loss in altitude ensues, with Mach number exceeding unity. Throughout most of this latter period, the pilot must have been unable to move the controls due to the very high stick forces needed to overcome the control-surface loadings, since the aircraft lost a total of 27,000 ft.

As an example of a low Mach number, low-altitude upset, contrary to upset A, consider another actual incident, upset B. In this case, the aircraft climbs through mild turbulence (0.25 peak g) for 40 sec, experiences increasing turbulence for 10 sec, then goes through a 30-sec period of violent pitching (5.8 g 's peak-to-peak), negative and positive stall, and a drop of 2800 ft from a peak altitude of 4000 ft. The Mach number remains below 0.5 throughout.

A primary common factor in upsets A and B is the occurrence of violent pitching involving negative stall at the moment of upset. Shock-induced stall might aggravate this condition, but it is not essential. The preliminary studies suggest that a severe, large-scale up- or down-draft may be the chief factor in turbulence upset. The ability to recover from such stringent maneuvers will depend largely on the position of the pitch-trim actuator¹ and the speed-altitude combination.

Featured Simulation

A study of an actual catastrophic incident, upset C, involving severe turbulence, provides interesting results as well as demonstrating the technique of simulation. The VGH flight record is available for comparison. The high, negative load factors, the corresponding structural failure, and the lack of information on the initial trim of the airplane makes this accident highly suitable for testing the capacity of the nonpiloted, purely analytical simulation to predict a probable sequence of events. From the variety of conditions that could be rationalized to explain the observed upset, one that is plausible follows from the simulation by iteratively varying the parameters. Rational amplitudes and frequencies of turbulence are postulated upon known data.⁵

Rates and amplitudes of control-surface motions are limited to values compatible with the Mach number and a reasonable pilot effort for the buffet environment present. Performance information is consistent with usual pilot technique for the given flight conditions, according to various sources including postaccident investigations.^{1,6,7} Airplane control and stability limitations are established from flight tests and manned, moving-base simulator studies.¹ According to these documents, all current, commercial, jet transports have very similar characteristics; therefore, the results of the present study are useful in understanding the basic phenomena common to nearly all of the jet-transport incidents.

Criterion: The primary, constraining criterion on the simulation is that it duplicate the VGH flight record of velocity, normal acceleration, and altitude while keeping within the bounds of the pilot effort (with the stick force including artificial feel) and the aircraft control-surface effectiveness (with Mach number dependency), according to the design specifications of the aircraft as well as studies[‡] like NASA's.¹ Also, the gust profile should be simple in form, but representative of the prevailing conditions of turbulence. Iterative variations of the pilot action and the gust profile yield acceptable and unacceptable variations under the criterion.

Pilot action: The pilot-action representation in the equations of motion is the most difficult and perhaps questionable segment of the calculations. Only fixed-base and "shake-chair" human-factors simulators were available at the time. The pilot-transfer-function approach⁸ used for quality-index studies is inadequate for discrete-time solutions; therefore, the only alternative was to program a direct, tabular chronicle of pilot action, guided by the probable pilot responses according to the investigations of Soderlind⁹ and Ashlock,² including the nonlinear manner in which this action affects control surfaces via control gain and artificial feel. Conceivably, an infinite number of actions are pos-

[‡] These studies sometimes are in disagreement with the manufacturer's claims, in which case the discrepancy must be resolved according to the investigator's judgment, generally giving preference to the more recent findings.

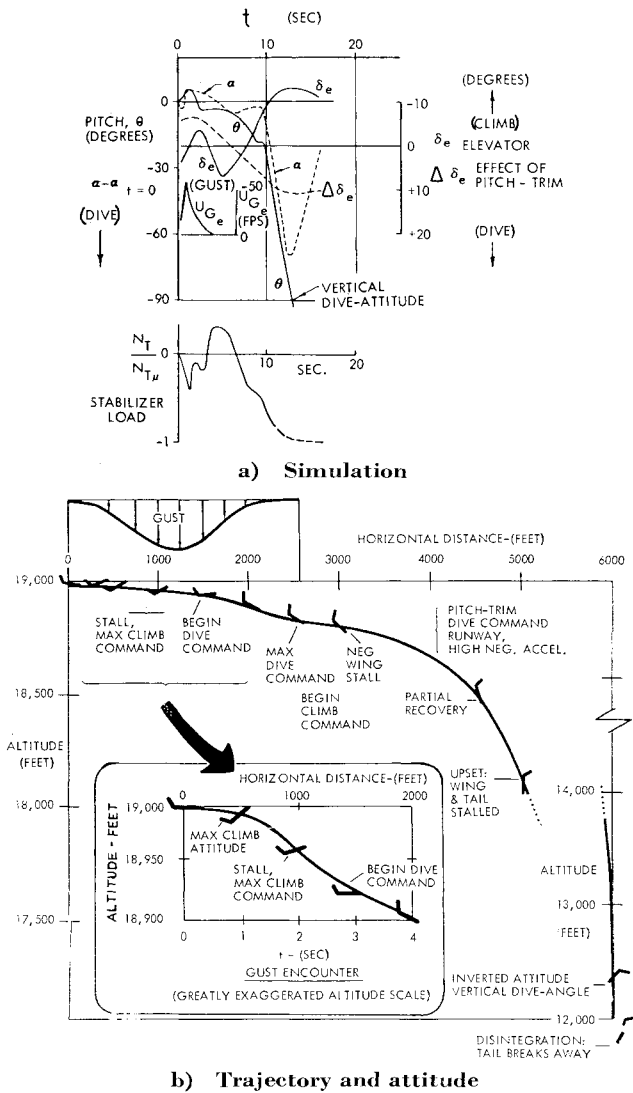


Fig. 5 Upset C.

sible; a unique prediction may, therefore, be infeasible. However, the preliminary studies and other studies^{9,10} that have since become available indicate that a similar sequence of events is common to most upsets, and that poor pilot practices and commonly unrecognized nonlinear aerodynamics at stall and in turbulence lead to a repetitive and predictable set of circumstances.

Gust hypothesis: The flight records show the transport climbing north at rates varying from 2000 to 7500 ft/min and Mach numbers near 0.5. At various intervals during the several minutes preceding upset, the pilot reports moderate-to-severe turbulence. Contrary to upset A, an analysis of the instantaneous lift coefficient shows no values approaching the buffet boundary. Thus, atmospheric turbulence is the most likely source of incipient excitation in this case.

For several minutes immediately prior to the zero time of Figs. 5 and 6, the transport climbs from 5000 to 19,000 ft, local thunderstorms are reported, and there is a general acceleration level of $\pm \frac{1}{4} g$. From the acceleration trace, it is estimated that, for approximately 20 sec immediately prior to zero time, there is a very long wavelength updraft upon which is superimposed a pilot-induced, $\frac{1}{7}$ -cps oscillation. A similar frequency has been observed in other upset records,¹¹ and seems to be a "hunting frequency" of the pilot when he is under duress. Penetrating the positive gradient of the gust results in some loss in altitude due to the inherent dive response of the airplane. The pilot, characteristically intent on recovering lost altitude,⁶ runs the pitch-trim actuator

to -4 points, which is equivalent in magnitude to more than 8° of elevator. He slightly relaxes the controls to compensate for the pitch trim. The combined effect of pitch trim and elevator control is to produce a small nose-up pitching of the airplane just as the gradient of the updraft drops to zero. The high, negative accelerations immediately after zero time can only be caused by a pronounced down-gust.

Although complex variations in the gust profile could possibly produce similar airplane gyrations and thus confound the results, such amplitude-wavelength combinations are highly improbable from the standpoint of the large number of upsets that occurred during the period 1962-1964. The procedure, therefore, is to choose the simplest profiles having a high likelihood of occurrence and to admit to further analysis only those which meet the aforesaid criterion. Thus, an investigation of the various wavelengths and amplitudes for 1-cos shaped gusts determines those combinations likely to produce the stalls observed in most incidents. The critical conditions in the present case are a downward gust with a 60-chord wavelength and a 70-fps amplitude, combined with another gust an order of magnitude less intense, superposed upon the first and sustained for 10 sec afterwards. This gust intensity is somewhat higher than the standard design gust of 50 fps. However, its probability of occurrence is higher because of its longer wavelength which corresponds to the short-period mode of the airplane, compared with the design-gust wavelength which corresponds more with wing-first-bending frequency.

Upset: The main gust lasts for 4 sec, including the indicial delay, but spends most of its force during the first 2 sec, during which the airplane pitches nose-upward, stalls, and remaining stalled, pitches nose-downward. Finally at this point the pilot reacts to the increasing strength of the normal acceleration and stall buffet. The combined pitch control he applies subjects the airplane to negative lift. The runaway pitch-trim actuator defeats the efforts of the pilot to recover by use of the elevator alone and establishes the characteristic irreversibility of the upset. Thus, the plane swings into a long, arcing dive, going into negative stall at 10 sec and a vertical dive attitude at 12 sec. At 14 sec the tail section fails.

Interpretation: It is neither practical nor desirable to carry through a detailed explanation of all possible causes and effects related to the complicated interactions of some 10 time-varying parameters. However, a few refinements to

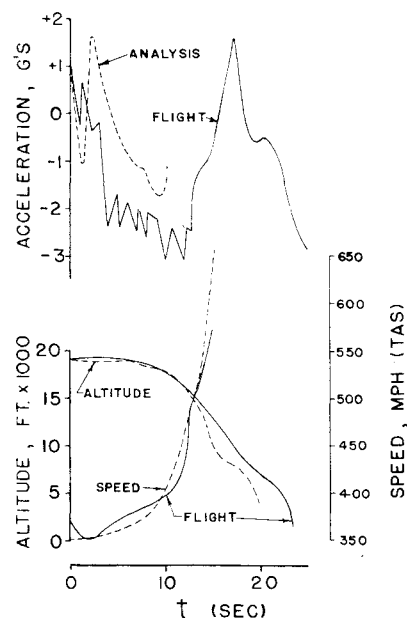


Fig. 6 Comparison with upset C flight record.

the foregoing bring out important characteristics which provide insight into the general upset problem.

As stated previously, at $t = 0$ (Figs. 5 and 6) the airplane is flying through a negative gust gradient which initiates a nose-up pitch rate. The stabilizer trim is changing to increase the rate of climb; the elevator is depressed to offset the stabilizer; and the net pitch control is zero but moving in the climb direction. The angle of attack corresponds to level flight at 19,000 ft.

At $t = 0.5$ the downward gust causes a negative angle of attack and pitch upward. At $t = 1.0$ the gust nears its peak. The airplane has rotated to a maximum climb attitude (Fig. 5b inset), and the angle of attack reaches the value for incipient stall. The stall, delayed by lift-lag and gust-gradient effects, takes place a second later.

By $t = 2.0$, the pilot senses the stall buffet and actuates the stabilizer trim at a rate of $1^\circ/\text{sec}$, surface nose-up (dive command, Fig. 5b), equivalent to $2^\circ/\text{sec}$ elevator. (This stall point is at the left end of the dashed line shown on the 1.5- g buffet boundary in Fig. 3.) He also applies additional dive command through the elevator in an attempt to regain the speed lost during the stall. This simultaneous actuation of control surfaces rapidly accelerates the downward pitching, resulting in high, negative g 's and turbulent buffeting. Although the pilot counters with the elevator, the net control-surface action increases the dive angle causing negative stall at 6 sec, as reckoned by comparing the pitch attitude (Fig. 5a) with the negative attitudes from the nonlinear lift characteristics (Fig. 7). Confused by the high negative- g buffeting, the pilot delays too long before applying negative elevator; speed and stick forces are now excessive. Whether through confusion of the pilot or mechanical malfunction, the pitch-trim actuator is not reversed, but continues in a runaway fashion to increase the airplane nose-down control force. Within seconds the indicated airspeed exceeds 400 knots at 14,000 ft, a condition beyond maximum dive velocity (Fig. 3). The pitch-trim-actuator drive stalls at approximately 4 points, surface leading-edge up, which is almost equivalent to the maximum elevator deflection available at this Mach number for most commercial jet aircraft.¹ Corresponding stick forces are estimated well in excess of 140 lb, and it is doubtful that the pilot was able to pull the airplane nose up.

Severe negative stall occurs again between 10 and 14 sec, during which the dive attitude and speed both accelerate rapidly until, at 14 sec, the airplane is vertical, although the flight-path angle is only -25° . At approximately 16 sec, the high, negative angle of attack and the greatly increased dynamic pressure at lower altitude results in horizontal-stabilizer forces estimated from profile drag characteristics to exceed ultimate load at an altitude somewhere below 12,000 ft. (The postaccident investigation located the tail section several miles from the scene of the primary impact.) The simulation was arbitrarily terminated prior to the estimated point of structural failure.

The inclusion of compressibility in the indicial lift functions throughout the preupset period is not believed to have had a great effect upon the basic response. However, the increased lag in lift buildup and the corresponding tendency to delay the apparent onset of lift-loss at stall, usually characterized by steady-state theory as more sudden, would tend to add to the pilot's confusion. During the upset, when buffeting and violent pitching may obscure the true attitude indication, an added fraction of a second of indecision as to the presence of stall can greatly increase the chances of being upset.

Study evaluation: The simulation is fairly realistic by comparison with the VGH records for altitude and speed, but unrealistic by comparison with the normal acceleration (Fig. 6). [The analytical acceleration is not shown past the time where large pitch angles prevent direct comparison of the vertical coordinate representation (plunge mode) of

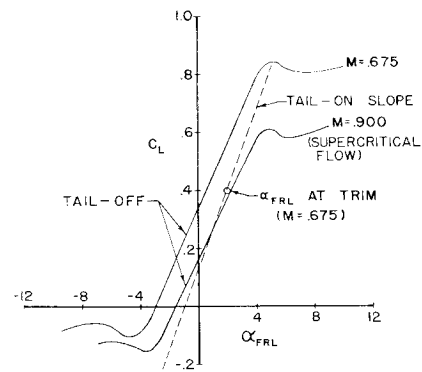


Fig. 7 Sample lift coefficient $C_L(\alpha)$.

the simulation program with the flight load factor. The measurements are always taken normal to the fuselage reference line, so the coordinates are not comparable for large pitch attitudes.] If a more complicated gust representation is used, such as additional high-intensity gusts superimposed on the relatively short wavelength gust used in the analysis, then even higher negative load factors might be induced. However, the primary purpose is not so much to simulate exactly a specific incident as to formulate a simple hypothesis that allows the simulation program to reproduce the general flight characteristics associated with turbulence upset. In this sense, the results confirm the feasibility of the method, since during the many simulated flights the same kind of upset could not be duplicated for significantly different variations in the gust profile without exceeding the bounds of pilot effort or control effectiveness. The use of the manufacturers' design data on control effectiveness failed to duplicate the upsets studied, whereas the use of the reduced effectiveness at high Mach number (approximately 50%) shown in the NASA/FAA studies¹ easily showed insufficient control to allow recovery for the same pilot action. The Boeing simulator studies, published in a trade journal¹⁰ long after the present studies were completed, show very similar hypothesized pilot action and aircraft response, including the negative stall, thus providing further confirmation of the validity of the simulation.

Compressibility Effects on Gust Loads

At the end of the simulation studies just described, a number of additional runs were made to study the effects of compressibility in the gust-load problem. The authors previously presented the data (Fig. 8 of Ref. 12) based on work initiated as early as 1961. This was given in the form of a plot of a gust-load-alleviation factor vs Mach number with several curves corresponding to various values of a mass parameter. Their conclusion indicated the possibility that the over-all Prandtl-Glauert correction applied to the incompressible gust-loads formula leads to conservative values of the load factor when compared to those based on the exact theory. In addition, the results emphasized the importance of compressibility in the upset simulations since these involved a similar type of transient-gust loading at Mach numbers from 0.4 to as high as 1.15, according to the VGH flight records. Since then, they have further investigated the gust-load problem by means of a Laplace-transform solution on the digital computer. The new data confirm both the results and conclusion from the original paper, and also serve to clarify the interpretation of those results as well as exposing an apparent need to update the present gust-load formula^{13,14} with a re-evaluation of VGH data.¹⁵

Civil and Military Specifications

The current military¹³ and civil¹⁴ specifications on the use of the gust-loads formula in the design of transport aircraft

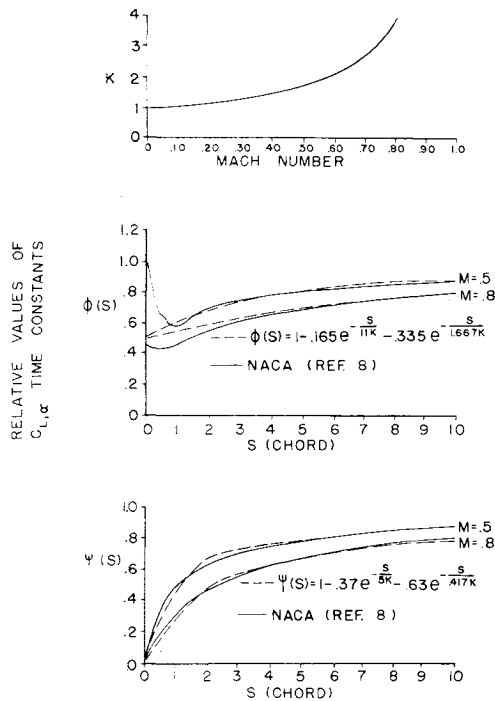


Fig. 8 Comparison of theoretical and approximate unsteady lift functions.

are practically identical. They stipulate a gust-load factor according to the formula $n = 1 + \rho_0 K_g U V a / (W/S)$, where U and V are in equivalent airspeed units. The incremental part of this factor is simply the maximum air load given by the sharp-edged-gust formula (or, equivalently, from steady-state aerodynamics for the given gust profile) multiplied by the so-called "alleviation factor" that Pratt and Walker¹⁵ define as $K_g = 0.88\mu / (5.3 + \mu)$, where μ is the mass parameter $\mu = (W/S) / \rho b a g$. Note that the normal-force-curve slope a also appears in μ . The specifications stipulate values of the derived gust velocity U for various flight conditions. This velocity is the amplitude of a 1-cos shaped transient gust whose wavelength is 25 chords. The important point here is that the original analysis by Pratt and Walker, which defines the alleviation factor and which thereby revises the original gust-load formula, is for incompressible flow. Furthermore, the agencies do not show in their standard specifications how to account for compressibility. This is perhaps surprising, since the basic effect of compressibility on gust loads was documented fifteen years ago by Lomax.¹⁶

Early Studies

The application of theoretical aerodynamics to the gust-loads problem in the regime of compressible flow was made by Bisplinghoff et al.¹⁷ in 1951. They were able to produce practical results only for supersonic speeds, however. In discussing the problem for the case of high subsonic speeds they pointed out the need to develop compressible lift-growth functions analogous to the Wagner function for incompressible flow and suggested that for Mach numbers below 0.6 the simple application of the Prandtl-Glauert correction to the lift-curve slope appearing in the mass parameter μ as well as in the expression for the load factor n might be sufficient. In an NACA Technical Note published at about the same time, Mazelsky¹⁸ computed the analogous Wagner function for the Mach number 0.7 by

means of the reciprocal relationship which exists between this indicial function and the oscillatory lift coefficient whose tabulated values were available. Although he could not obtain the analogous Küssner function in this way, he developed an approximate calculation and estimated a part of it. From his results, Mazelsky concluded that since the lift growth is less at $M = 0.7$ than at $M = 0.0$, then the gust-load factor obtained by applying an over-all Prandtl-Glauert correction to the incompressible indicial lift functions (as suggested by Bisplinghoff et al.) would probably be higher than the exact theoretical value at the higher subsonic speeds. During the next two years Lomax et al.^{16,19} developed and applied a direct method for evaluating the lift-growth functions required to handle the transient-gust problem in subsonic, compressible flow. Lomax¹⁶ gives specific results for sharp-edged and triangular gusts for various mass parameters, including the subsonic Mach numbers, 0, 0.5, and 0.8, which are of interest here.

1-Degree-of-Freedom Transient-Gust Response for Unsteady Compressible Subsonic Flow and a 1-Cos Shaped Gust

The present formulation corresponds to a discrete-gust model (cf. Pratt and Walker) in which the aircraft is regarded as a rigid wing free to translate vertically. The wing is thin, has a chord of $2b$, an infinite aspect ratio, and a constant forward speed V . The discrete gust has a 1-cos shape and a wavelength of 25 chords. Since the effects of planform geometry are not of primary interest here, only the two-dimensional case is considered. Then the governing equation for the response may be written:

$$M_w d^2 \xi / dt^2 = l_G + l_M \quad (1)$$

where M_w is the wing mass, $d^2 \xi / dt^2$ the vertical acceleration, and l_G and l_M the lifts per unit span due to the gust and the resulting motion, respectively. Introduce the dimensionless time variable $s = Vt/2b$, which is the distance traveled in chords, define a modified Küssner function $\psi(s)$, which depends on Mach number so as to account for compressibility effects, and use the superposition integral to express the lift:

$$l_G(s) = \beta^{-1} a \rho V b \int_0^s w_G(\sigma) \psi'(s - \sigma) d\sigma \quad (2)$$

where $w_G(\sigma)$ is the vertical gust velocity. Similarly define a modified Wagner function $\phi(s)$, etc.:

$$l_M(s) = -\beta^{-1} a \frac{1}{2} \rho V^2 \left[\frac{1}{4} \beta \xi''(s) + \int_0^s \xi''(\sigma) \phi(s - \sigma) d\sigma \right] \quad (3)$$

The prime indicates differentiation, $\beta = (1 - M^2)^{1/2}$ where M is the Mach number and $a = 2\pi$ is the incompressible steady-state lift-curve slope. (For details on the development of these forms for $M = 0$, see Bisplinghoff et al.²⁰) Note that $d^2 \xi / dt^2 = (V^2/4b^2) \xi''(s)$, substitute (2) and (3) into (1), take the Laplace transform of the result, and solve for the response transform-variable:

$$\bar{\xi}(p) = \frac{2b}{p} \frac{\bar{w}_G(p)}{V} \frac{\bar{\psi}(p)}{\beta(\mu + \frac{1}{4}) + \bar{\phi}(p)} \quad (4)$$

where the bar indicates that the Laplace transform has been taken, whence the transform variable p replaces s . Approximate the function $\psi(s)$ by the two-exponential-term expression developed at Caltech and modified by a time-constant factor K as indicated by Wilts²¹:

$$K(s) \cong 1 - 0.37e^{-s/5K} - 0.63e^{-s/417K} \quad (5)$$

Similarly, approximate $\phi(s)$ by the expression of R. T. Jones²² as modified by the same time-constant factor:

$$\phi(s) \cong 1 - 0.165e^{-s/11K} - 0.335e^{-s/1.667K} \quad (6)$$

§ Some consideration of this is frequently arranged through unilateral agreement or arbitration on the design requirements.

where $K = 1 + 2.18M^2\beta^{-3/2}$ and the comparisons of (5) and (6) with the results of Lomax¹⁶ are shown in Fig. 8. Note that the factor K wholly accounts for the influence of the Mach number on the values of $\psi(s)$ and $\phi(s)$. For the 1 - cosine gust,

$$w_G(s) = \frac{1}{2}U[1 - \cos(2\pi s/25)][u(s) - u(s - 25)] \quad (7)$$

where $u(s) = 0$ for $s < 0$, 1 for $s > 0$. Transform (5-7), substitute into (4), and solve for the acceleration:

$$\ddot{\xi}(s) = \frac{0.792}{(\mu + 1/4)K} \left(\frac{2\pi}{25}\right)^2 \frac{UV}{2b\beta} \mathcal{L}^{-1} \left\{ \frac{M(p)}{N(p)} (1 - e^{-25p}) \right\} \quad (8)$$

where

$$M(p) = (p + 1/11K)(p + 1/1.667K)(p + 1/3.304K) \quad (8a)$$

$$N(p) = (p + 1/5K)(p + 1/0.417K)(p^2 + (2\pi/25)^2 \times (p^3 + a_2p^2 + a_1p + a_0)) \quad (8b)$$

$$a_0 = 0.0545454/K^2\beta(\mu + 1/4) \quad (8c)$$

$$a_1 = 0.0545454/K^2 + 0.561454/K\beta(\mu + 1/4) \quad (8d)$$

$$a_2 = 0.690909/K + 1/2\beta(\mu + 1/4) \quad (8e)$$

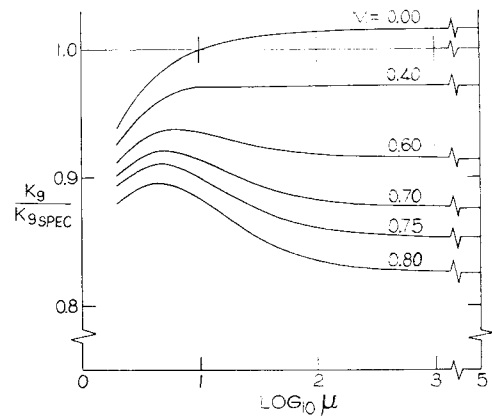
Results

Figure 9 shows the results from a digital computer solution²³ of (8). The alleviation factor K_g is the maximum value of the acceleration ratio $K_g = \max[\ddot{\xi}(s)/\ddot{\xi}_{ss}]$, where $\ddot{\xi}_{ss}$ is the hypothetical acceleration due to a vertical gust velocity U according to steady-state (subscript "ss") aerodynamics, neglecting the effect of the ensuing motion. That is, $\ddot{\xi}_{ss} = (a/\beta)(U/V)(2b)(\rho V^2/2)M_w = UV/2\mu b\beta$. Normalize (8) in this manner, then the expression,

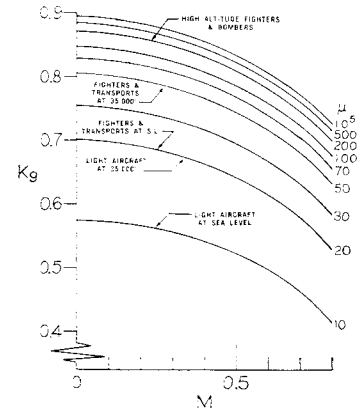
$$K_g = \left(\frac{\ddot{\xi}(s)}{\ddot{\xi}_{ss}}\right)_{\max} = \frac{0.792}{K} \frac{\mu}{\mu + 1/4} \times \left(\frac{2\pi}{25}\right)^2 \left[\mathcal{L}^{-1} \left\{ \frac{M(p)}{N(p)} (1 - e^{-25p}) \right\} \right]_{\max} \quad (9)$$

gives the alleviation factor which Fig. 9b presents as a function of the parameters M and μ . Now follow the earlier suggestion for obtaining the alleviation factor for the compressible case by applying the Prandtl-Glauert correction to the lift-curve slope in the incompressible gust-load formula which the civil and military specifications quote; then the alleviation factor is $K_{g_{spec}} = 0.88\mu\beta/(5.3 + \mu\beta)$. Figure 9a compares the theoretically exact values of K_g with the approximation $K_{g_{spec}}$. At the Mach number $M = 0.8$ and the mass parameter $\mu = 100$, the figure shows that the factor $K_{g_{spec}}$ is conservative by about 18%. It is of interest to note that for these same values, $M = 0.8$ and $\mu = 100$, Lomax's results¹⁶ (Lomax's μ is 2π times ours) for a triangular gust whose wavelength is 24 chords shows that the alleviation factor K_g is about 18% lower than its corresponding value at $M = 0$, as compared to 20% according to the present results for the 1 - cos gust.

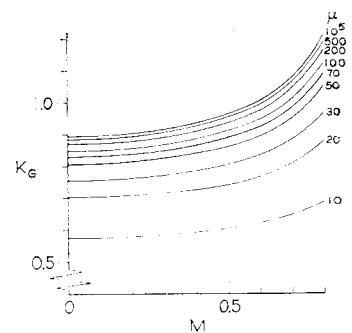
The definition of K_g specifies a reference acceleration which is dependent upon the Mach number and consequently might lead to a misconstruing of the results of Fig. 9b. Perhaps a more satisfactory definition of the alleviation factor is to use for the reference acceleration the incompressible steady-state value $\beta\ddot{\xi}_{ss} = a(U/V)(2b)(\rho V^2/2)/M_w$, which is independent of Mach number. Then the new alleviation factor K_G accounts for the whole combined effect of unsteadiness and compressibility. It is related to the first one by the simple formula $K_G = K_g/\beta$ and is shown in Fig. 9c. In terms of this new value, the gust-load factor is $n = 1 + \rho_0 K_G UV a/2(W/S)$, where the symbols are as defined before, and the normal-force-curve slope a again is its incompressible,



a) Alleviation factor compared with values obtained by Prandtl-Glauert correction



b) Alleviation factor



c) Modified alleviation factor

Fig. 9 Compressibility effects on gust loads.

steady-state value. The plot of K_G reflects the predominant Prandtl-Glauert effect which increases the load at the higher Mach numbers. It also reflects the considerable mitigation of the Prandtl-Glauert effect due to the combination of unsteadiness and compressibility. For example, the load increases at $M = 0.8$ only 25% over the value at $M = 0$ for $\mu = 100$ as compared to 67% according to the Prandtl-Glauert correction for the steady-state effect.

In comparing these newer results with the older ones from the simulation program,¹² the agreement is within 10% for the lowest mass parameter at $M = 0.8$, within 5% for $\mu > 20$ and $M < 0.6$, and within 1% for $\mu > 100$ at all M or $\mu > 20$ for $M = 0$. This sort of agreement is rather good corroboration of the earlier results since those were for a finite aspect ratio of 9 and a sweep angle of 25°.

In principle, the results of Fig. 9a for $M = 0.00$ should show perfect agreement, i.e., $K_g/K_{g_{spec}} = 1.0$ for all values of μ . The discrepancies are attributed almost entirely to the difference in the series approximation to the Küssner function. The present representation has two exponential terms and, in the critical range of the independent variable, is generally about 2.6% higher than the more accurate three-term approximation of Pratt and Walker.¹⁵ The present

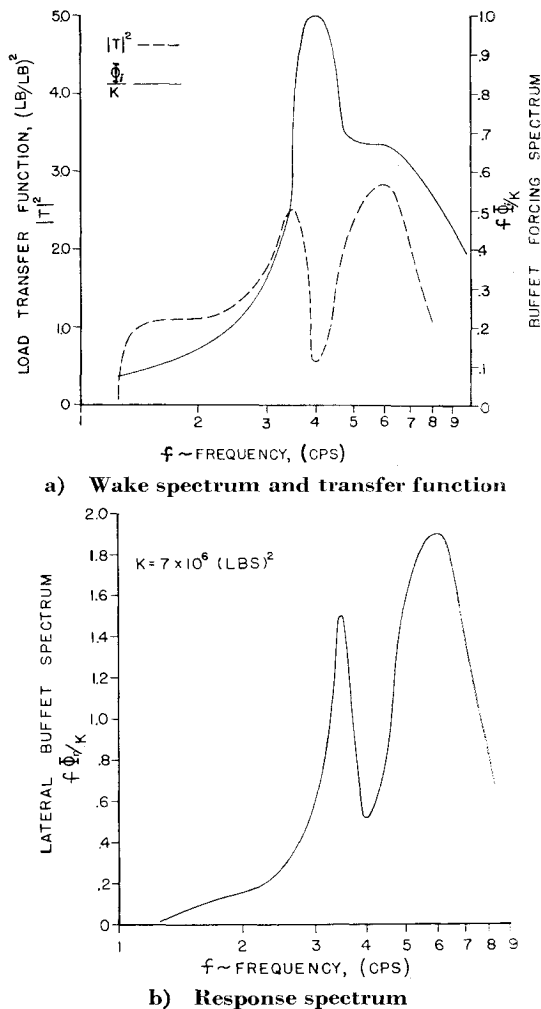


Fig. 10 Fuselage autobuffet.

results therefore do not show the alleviation factor evaluated for $\mu < 10$. The chief difference in the results is, then, that the present values of K_g are asymptotic to 0.895 for large values of μ , whereas the results of Pratt and Walker indicate an asymptotic value of 0.88, giving rise to the discrepancy of 1.7% ($K_g/K_{g\text{spec}} = 1.017$) shown in Fig. 9a for large values of μ at $M = 0.00$. The representation of the Wagner function here is the same as that of Pratt and Walker; hence, there should be no other source of discrepancy except for the slight differences arising from the use of different methods of solution.

Fuselage Autobuffet

Problems of bodies embedded in turbulent wakes generally are intractable by purely analytical methods, at least for accurately determining structural loads. Therefore, the problem is usually solved semiempirically²⁴; however, in any specific buffet condition for which the power spectral density of turbulence energy can be predicted, the simulation analysis described herein is capable of producing the corresponding structural response, simply by virtue of its capacity to compute the required transfer function.

A wake, containing a clearly defined spiral vortex-sheet, exists behind fuselage-shaped bodies inclined to a flow and produces strong, periodic pressure fluctuations transverse to the primary flow and varying with incidence.^{25,26} This has been discussed in connection with the wake behind aircraft with highly swept aft fuselages, where it is shown that vortices are generated after the flow separation lines along the

fuselage sidewall.²⁶ The strength of these vortices is augmented by increasing the fuselage upsweep and is further related to the turbulence intensity in the wakes of bluff contours like the protuberant fairing over wheel wells. The wing downwash field draws this turbulent energy into the near wake of the aft fuselage. There is the tendency for the waxing of vortices to a critical strength followed by abrupt shedding,²⁷ analogous to the production of the classical von Kármán street. However, the upwash beneath the center of the afterbody removes a large portion of the circulation energy causing the formation of a relatively stationary pair of spiral vortex sheets which have antisymmetrically, periodically fluctuating lines of separation on either side of the body. As a result, the rms lift coefficient of the fuselage is only one-third of its classical value of 0.13.²⁶ Although some development of turbulence is anticipated at supercritical Reynolds numbers,²⁸ a characteristic periodicity persists throughout this regime of flow.²⁷ Strong periodicity is also measured in cylindrical wakes at "hypercritical" Reynolds numbers ≥ 3.5 million.^{29,30}

Analysis

This analysis presumes knowledge of the fuselage cross-flow wake spectrum. Assume that the energy spectrum can be based on measurements of a turbulent wake below a fuselage-type body. Such data are obtained from measurements made in the cross-flow wake induced by dive brakes extended at various angles from a fuselage-type body.³¹ Although those tests were idealizations of a different buffet problem (dive brakes) and the Reynolds numbers were only 10 to 20% of our full-scale flight values, no other pertinent data appear to be available in the required power-spectral form. Moreover, experimental evidence indicates that the periodic wake character is not markedly different for wide variations in bluff-body shapes^{32,33}; and, as mentioned, strong periodicity still persists at high Reynolds numbers.^{29,30} The energy spectrum is approximately established as follows. The isotropic component of turbulence present in the wake is accurately predicted using the von Kármán spectrum formula with the scale of turbulence based on the body width.³⁴ Root-mean-square velocities correlate well using data for fluctuating lateral lift coefficients from high Reynolds number tests of fuselage-fin bodies.²⁵ The effects of body incidence on the Strouhal frequency can be determined from the crosswise component of flow and the local downwash angles.³⁵ The corresponding pressure and force fluctuations are adjusted according to the appropriate lift coefficient²⁶ (see preceding discussion) to obtain an input power spectrum Φ_i (Fig. 10a). The nearly periodic component is obtained from estimates³⁴ based on experimental measurements³¹ that show such a component to appear near the Strouhal frequency and to contain about 10% of the total turbulence energy. Also, at high Reynolds numbers the shed-vortex energy is relatively constant in the range of fuselage incidences of interest.²⁵ The fuselage transfer function squared $|T|^2$ (Fig. 10a) is obtained in terms of structural lateral load per unit lateral-lift-force excitation. The magnitude is computed using total-airplane, flexible asymmetric modes having dominant fuselage response amplitudes. The response power spectrum Φ_r (Figure 10b) is the product of the two functions, Φ_i and $|T|^2$ (Fig. 10a) retaining the appropriate normalizing factor K . The rms responses are obtained by integrating the response power spectra.

Flight-Test Comparison

A phenomenon similar to that described previously has been observed on jet-transport aircraft during early flight tests. The data were difficult to obtain because of the intermittent occurrence of the phenomenon and the relatively low energies of excitation experienced. However, from the most severe instances recorded, the dominant frequencies are 4

and 7 cps, showing both damping and frequency characteristics in agreement with the present results (Fig. 10). The analysis predicts the largest motion to be $\frac{1}{4}$ -in. peak-to-peak lateral amplitude at the base of the vertical fin, a value that corresponds to the amplitude observed on the airplane during the most severe occurrence. The phenomenon is an example of a nonclassical buffet, although like the classical examples, there did appear to be some dependence on dynamic pressure.

Subsequent flight tests with repaired wing-root and wheel-well intersections with the fuselage eliminated the buffet, according to flight reports. This probably resulted because of reduced turbulent flow entrainment within the rather thick boundary layer present on the aft fuselage of such large aircraft, thus removing the major source of vorticity propagation required for the generation of a vortex wake.

Past studies indicate that a small-amplitude, 4-cps vibration, present on most of the commercial jet-transport aircraft, is a characteristic fuselage frequency; this frequency is particularly detrimental from a human factors viewpoint.^{1,7} Acceleration levels from 0.2 to 0.5 *g* greatly decrease pilot proficiency if sustained for several minutes at this frequency. These levels are considerably in excess of those found in this study.

Conclusions and Recommendations

A program of analysis has been applied to an actual case of turbulence upset, and to the related problems of compressibility effects on gust loads and fuselage autobuffet.

Turbulence Upset

Previous results from piloted simulators and flight tests can be substantiated and augmented by the iterative operation of a nonpiloted, computer-simulation program which contains all of the characteristics pertinent to the problem. For realistic simulation, nonlinear aerodynamic characteristics, including both positive and negative stall, and accurate pitch-trim and control-surface rates of application and amplitude must be considered, and should be based on flight tests where practicable. Specifically: 1) under certain conditions, including an adverse pitch-trim, a downward gust of wavelength corresponding to the pitch frequency is likely to develop into a maneuver-upset condition for gust intensities with relatively great likelihood of occurrence; 2) under similar conditions of gust wavelength, pilot action to maintain altitude rather than attitude while penetrating moderate-to-severe turbulence can easily produce divergent pitching oscillations; 3) shock-induced boundary-layer separation is a contributing factor in the development of violent pitching oscillations at high altitude and high Mach number, but is not generally essential in causing an upset; 4) pilot disorientation in high load-factor buffet, instrumentation readability, high stick-force requirements, and other human factors all contribute to upset, particularly in inhibiting the pilot from making correct decisions relative to pitch trim, flight speed, and attitude control; and 5) nonlinear aerodynamics and control characteristics, particularly both positive and negative stall, must be included in a simulation of turbulence upset.

Compressibility Effects on Gust Loads

A theoretically exact analysis of the compressible gust-load problem lends support to the general contention that the gust-load formula commonly used in preliminary design analysis needs revision. In particular:

1) According to the results (Fig. 9a) the over-all Prandtl-Glauert correction applied to the incompressible gust-loads formula leads to conservative values of the load factor when compared to those based on the exact theory. This seems

to be most significant for the heavier aircraft in the transport category.

2) If a gust-load formula is to be used, then the use of an alleviation factor such as that given by the results in Fig. 9b, or equivalently, 9c, with a re-evaluation of VGH data would seem to yield a more rational basis for establishing the design criteria for modern, high-speed jet transports, rather than the presently applied gust-load alleviation factor which is strictly valid only for the case where compressibility effects are negligible.

Fuselage Autobuffet

A program of analysis can be devised to analyze the problem rather simply and still gain realistic responses for a given aircraft. Thus, *g*-seat simulators simultaneously employed with a real-time, rational, dynamic analysis can be useful in studying the attendant effects of pilot annoyance, disorientation, or difficulty of instrumentation read-out.

References

- ¹ Sadoff, M., Bray, R. S., and Andrews, W. H., "Summary of NASA Research on Jet Transport Control Problems in Severe Turbulence," *Journal of Aircraft*, Vol. 3, No. 3, May-June 1966, pp. 193-200.
- ² Ashlock, J. R., "Jet Turbulence Problems—Part 1: Detection, Flight Procedures Emphasized," *Aviation Week & Space Technology*, Vol. 80, No. 7, Feb. 17, 1964, pp. 38-41; also, "Jet Turbulence Problems—Part 2: Forecasting Methods Gradually Improve," Vol. 80, No. 8, Feb. 24, 1964, pp. 45, 46.
- ³ Theisen, J. G., "Turbulence/Upset Problems of Jet Transports," Research Memo. ER-8356, May 1966, Lockheed-Georgia Co., Marietta, Ga.
- ⁴ Gray, W. L. and Schenk, K. M., "A Method for Calculating the Subsonic Steady-State Loading on an Airplane with a Wing of Arbitrary Plan Form and Stiffness," TN 3030, Dec. 1953, National Advisory Committee for Aeronautics, Washington, D.C.
- ⁵ Hart, J. E., Adkins, L. A., and Lacau, L. L., "Stochastic Disturbance Data for Flight Control System Analysis," ASD-TDR-62-347, Sept. 1962, Air Force Systems Command, Wright-Patterson Air Force Base, Ohio.
- ⁶ Soderlind, P. A., "Jet Turbulence Penetration," *Flight Standards Bulletin* 8-63, Nov. 12, 1963, Northwest Airlines Inc.; also, "Jet Transport Operation in Turbulence," Paper 64-353, 1964, AIAA.
- ⁷ Holland, C. L., "Performance and Physiological Effects of Long-Term Vibration," USAF: AMRL-TR-66-145, Oct. 1966, Aerospace Medical Research Lab., Wright-Patterson Air Force Base, Ohio.
- ⁸ Taylor, L. W., Jr. and Day, R. E., "Flight Controllability Limits and Related Human Transfer Functions as Determined from Simulator and Flight Tests," TN D-746, May 1961, NASA.
- ⁹ Civil Aeronautics Board, "CAB Accident Investigation Report: Turbulence Cited in Eastern DC-8 Crash," *Aviation Week & Space Technology*, Sept. 12, 1966, pp. 123-156.
- ¹⁰ Civil Aeronautics Board, "CAB Accident Investigation Report—Part 1: Vertical Air Drafts Cited in 720B Crash," *Aviation Week & Space Technology*, Aug. 16, 1965, pp. 104-119; also, "CAB Accident Investigation Report—Part 2: Study Adds Data on Control in Turbulence," Aug. 23, 1965, pp. 93-107.
- ¹¹ Perry, D. H. and Burnham, J., "A Flight Simulation Study of Difficulties in Piloting Large Jet Transport Aircraft through Severe Atmospheric Disturbances," TR 65195, Sept. 1965, Royal Aircraft Establishment, Great Britain.
- ¹² Theisen, J. G. and Haas, J., "Turbulence/Upset Studies on Jet Transports," Paper 66-1002, 1966, AIAA.
- ¹³ "Airplane Strength and Rigidity—Flight Loads," Military Specification MIL-A-8861, May 18, 1960. Aeronautical Standards Group.
- ¹⁴ "Airworthiness Standards, Transport Category Airplanes," *Federal Air Regulations*, Pt. 25, Nov. 3, 1964.
- ¹⁵ Pratt, K. G. and Walker, W. G., "A Revised Gust-Load Formula and a Re-evaluation of V-G Data Taken on Civil Transport Airplanes from 1933 to 1950," Rept. 1206, 1954, Langley Aeronautical Lab., NACA, Langley Field, Va.

¹⁶ Lomax, H., "Lift Developed on Unrestrained Rectangular Wings Entering Gusts at Subsonic and Supersonic Speeds," Rept. 1162, 1954, Ames Aeronautical Lab., NACA, Moffett Field, Calif. (supersedes NACA TN 2925, 1953).

¹⁷ Bisplinghoff, R. L., Isakson, G., and O'Brien, T. F., "Gust Loads on Rigid Airplanes with Pitching Neglected," *Journal of the Aeronautical Sciences*, Vol. 18, No. 1, Jan. 1951, pp. 33-42.

¹⁸ Mazelsky, B., "Numerical Determination of Indicial Lift of a Two-Dimensional Sinking Airfoil at Subsonic Mach Numbers from Oscillatory Lift Coefficients with Calculations for Mach Number 0.7," TN 2562, Dec. 1951, Langley Aeronautical Lab., NACA, Langley Field, Va.

¹⁹ Lomax, H. et al., "Two- and Three-Dimensional Unsteady Lift Problems in High-Speed Flight," Rept. 1077, 1952, Ames Aeronautical Lab., NACA, Moffett Field, Calif.

²⁰ Bisplinghoff, R. L., Ashley, H., and Halfman, R. L., "Dynamic Response to a Discrete Gust," *Aeroelasticity*, 1st ed., Addison-Wesley, Cambridge, Mass., 1955, pp. 673-679.

²¹ Wilts, C. H., "Aerodynamic Forces in Analog Computation," TR 116, Sept. 1959, California Institute of Technology Computing Center, Pasadena, Calif.

²² Jones, R. T., "The Operational Treatment of the Non-Uniform-Lift Theory in Airplane Dynamics," TN 667, Oct. 1938, Langley Memorial Aeronautical Lab., NACA, Langley Field, Va.

²³ Haas, J., "Compressibility Effects on Gust Loads at Subsonic Speeds," Research Memo. ER-9669, Dec. 1967, Lockheed-Georgia Co., Marietta, Ga.

²⁴ Byrnes, A. L., Hensleigh, W. E., and Tolve, L. A., "Effect of Horizontal Stabilizer Vertical Location on the Design of Large Transport Aircraft," *Journal of Aircraft*, Vol. 3, No. 2, March-April 1966, pp. 97-104.

²⁵ Stone, R. W. and Polhamus, E. C., "Some Effects of Shed Vortices on the Flow Fields around Stabilizing Tail Surfaces," Rept. 108, April-May 1957, NATO Advisory Group for Aeronautical Research and Development, Paris, France.

²⁶ Wickens, R. H., "Observations of the Vortex Wake of a Lifting Fuselage Similar to Those on Rear-Loading Transport Aircraft," Rept. LR-395, Aug. 10, 1964, National Research Council of Canada.

²⁷ Theisen, J. G., "Vortex Periodicity in Wakes," Paper 67-34, 1967, AIAA.

²⁸ Fung, Y. C., "Fluctuating Lift and Drag on a Cylinder in a Flow at Supercritical Reynolds Numbers," *Journal of the Aerospace Sciences*, Vol. 27, No. 11, Nov. 1960, pp. 801-814.

²⁹ Roshko, A., "Experiments on the Flow past a Circular Cylinder at Very High Reynolds Number," *Journal of Fluid Mechanics*, Vol. 10, Pt. 3, May 1961, pp. 345-356.

³⁰ Reed, T. G., "Ground Winds and Space Vehicles," *Astronautics and Aeronautics*, Vol. 3, No. 12, Dec. 1965, pp. 38-41.

³¹ Fail, R., Owen, T. B., and Eyre, R. C. W., "Preliminary Low Speed Wind Tunnel Tests on Flat Plates and Air Brakes: Flow, Vibration and Balance Measurements," C. P. 251, TN Aero. 2356, Jan. 1955, Royal Aircraft Establishment, Great Britain.

³² Prandtl, L. and Tietjens, O. G., *Applied Hydro- and Aero-mechanics*, Dover, New York, 1934, Plates 24-26, pp. 303-305.

³³ Roshko, A., "On the Wake and Drag of Bluff Bodies," *Journal of the Aeronautical Sciences*, Vol. 22, No. 2, Feb. 1955, p. 124.

³⁴ Taylor, J., "Buffeting Turbulence," *AGARD Manual on Aircraft Loads*, Pergamon, New York, 1965, pp. 245-260.

³⁵ Chiu, W. S. and Lienhard, J. H., "On Real Fluid Flow over Yawed Circular Cylinders," *Transactions of the ASME, Journal of Basic Engineering*, Vol. 90, Ser. D, No. 1, Jan. 1968, pp. 1-7.